Improving Control Accuracy of Steel Plate Temperature by Accelerated Cooling with Columnar Water Jets

Takahiro OHARA*1, Keiichi YAMASHITA*1, Kiichiro TASHIRO*2, Kensuke UENISHI*3, Taketsugu OSAKA*4, Dr. Masahiko MITSUDA*5

*1 Process Engineering Development Section, Research & Development Laboratory, Iron & Steel Business
*2 Sheet & Plate Products Development Department, Research & Development Laboratory, Iron & Steel Business
*3 Plate Production Department, Kakogawa Works, Iron & Steel Business
*4 Production Systems Research Laboratory, Technical Development Group
*5 Kobelco Research Institute, Inc.

The amount of cooling water, which affects the heat transfer characteristics, and the height of residual water on the steel plate surface, the height that changes in accordance with the steel plate size, were modeled for the accelerated cooling of steel plates with cylindrically-arranged multi jet. In addition, the heat transfer characteristics associated with the height of residual water were investigated by laboratory experiments to model the heat transfer coefficient, which is an index of heat transfer characteristics. Furthermore, the heat transfer coefficient model was optimized by the actual temperatures measured at multi-points on a steel plate in an actual machine, which enabled the accurate prediction of the plate temperature. A water flow rate control function was newly developed on the basis of the temperature prediction results and was introduced into the actual machine, which improved the accuracy of the plate temperature control.

Introduction

In the cooling step of the thermo-mechanical control process (TMCP),[1] a typical process for producing steel plates, each steel plate must be cooled uniformly at a desired cooling rate (CR) to a finishing cooling temperature by an accelerated-cooling device to realize the target material structure and properties. In the cooling control, it is necessary to consider how the flow and boiling mode of cooling water affect the heat transfer characteristics, so as to properly set the longitudinal and width directions of the steel plate and the cooling water flow on its upper and lower surfaces. Several steel plate producers have also developed cooling devices and cooling control technologies to more accurately control the steel plate in the cooling process.[2), 3)] The flow rate control sets the required cooling water flow rate on the basis of the calculated predictive values of the temperature of a steel plate in the cooling process. This means that the accuracy of the predictive calculation affects the accuracy of the temperature control.

Hence, Kobe Steel focused on the behavior of the cooling water on the upper surface of a steel plate, which affects the characteristics of heat transfer between the cooling water and the steel plate. In order to improve the accuracy of the predictive calculation, a prediction model was constructed for the height distribution of cooling water accumulated on the upper surface of a steel plate (hereinafter referred to as "residual water"). A heat transfer model taking into account the height of the residual water was constructed as well. Moreover, the constructed models were optimized and adapted for the cooling control of the actual machine to improve the accuracy of the temperature control of the steel plate.

This paper relates to the construction of a heat transfer model and describes the construction of a prediction model for the height distribution of residual water on the upper surface of a steel plate and the effect of the residual water height on the heat transfer characteristics. Also introduced are the results of evaluating the accuracy of the newly constructed heat transfer model.

1. Temperature prediction of steel plates in cooling process

For predicting the steel plate temperature in the cooling process, the steel plate temperature on the entrance side of a cooling header (start cooling temperature, hereinafter referred to as "SCT") is regarded as the starting point for predicting the steel plate temperature on the exit side of the cooling header (finishing cooling temperature, hereinafter referred to as "FCT"). In the cooling control, the calculated predictive value of the steel plate temperature is used as the basis for determining the flow rate of cooling water and other parameters that satisfy the desired FCT and CR. At this time, it is necessary to ensure the accuracy of the heat transfer model used in the predictive calculation. The heat transfer characteristics between the cooling-target surface (of a steel plate) and the cooling water vary greatly depending on the amount of cooling

water, its flow on the upper surface of the steel plate, the changes in boiling mode, the cooling water temperature and the surface texture of the steel plate.[4] In particular, the flow of cooling water on the upper surface of a steel plate is considered to vary greatly in accordance with the cooling conditions (size of the steel plate, water flow, and the like). Hence, a small testing machine simulating the actual cooling header was used to observe the flow of cooling water to develop a model for predicting the height distribution of cooling water staying on the upper surface of the steel plate. In the meantime, a cooling experiment was conducted to study the effect of residual water heights on the heat transfer characteristics and to develop a heat transfer model taking into account the height of residual water. Moreover, actual temperatures were measured at multi points in the cooling process to adjust the model parameters so as to optimize the heat transfer model being developed.

1.1 Model for predicting height of residual water on upper surface of steel plate

The cooling header used for cooling the upper surfaces of steel plates in Kobe Steel's steel plate mill comprises a repeated arrangement of a nozzle injection part for injecting high-pressure cooling water from densely disposed columnar water jets nozzles and an injection part without any nozzle. The heat-transfer coefficient during water cooling is affected by the flow state of the cooling water staying on the upper surface of the steel plate. Hence, the flow state of cooling water was examined by a cooling water flow observation test was performed.

Fig. 1 depicts the outline of the test, and **Fig. 2** shows the flow state of the cooling water on the upper surface of a steel plate during the test. The testing apparatus consists of a cooling header with a group of columnar water jets nozzles and an acrylic plate simulating a steel plate (hereinafter referred to as a "simulation plate") disposed under the header, while a half-width model was used in consideration of symmetry. An acrylic wall plate is placed at the symmetry boundary plane, and residual water is discharged from the end of the simulation plate. In order to observe the flow of residual water, the simulation plate and wall plate are made transparent. In this cooling water flow observation test, the distance between the nozzle tip and the simulation steel plate was 300 mm, the nozzle diameter was 3 mm, the nozzles were 500 jets/m^2, and the header size was 1,000 × 2,000 mm. The flow of residual water varies depending on

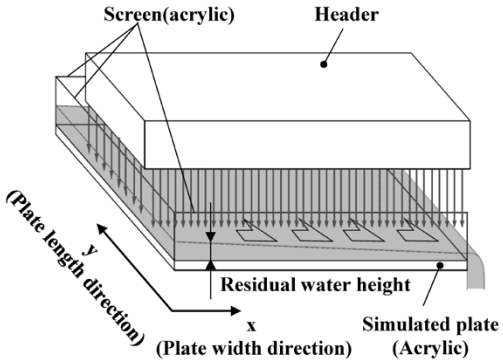

Fig. 1 Schematic diagram of test for observing flow of cooling water

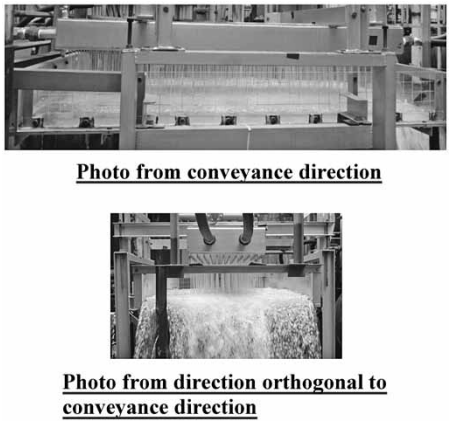

Fig. 2 Columnar water jets and residual water flow in experiment

the cooling water flow per unit area (water flow density) and the plate width. For this reason, the water density was set to 3 levels, the widths of the simulation plates were 1,500 mm and 2,000 mm, and the length was 1,000 mm. The distribution in the width direction of the residual water height was measured, and the results are shown in **Fig. 3**. The residual water height increases with increasing water flow density and plate width. On the other hand, the residual water height decreases from the center of the plate width toward the end of the plate width. From these results, the heat transfer characteristics are considered to change depending on the plate width, water flow density, and position on the plate surface.

Hence, the residual water height distributions were measured while changing the water flow density and plate width and, on the basis of the results, a model was developed to predict the residual water height at any position on the steel plate (**Fig. 4**). Here, the plate width direction is the x-axis, the plate longitudinal direction is the y-axis, the nozzle region length is a, the plate width is b, and the non-nozzle region length is c. Taking into account the symmetry, a 1/4 region for each was used as an analysis region.

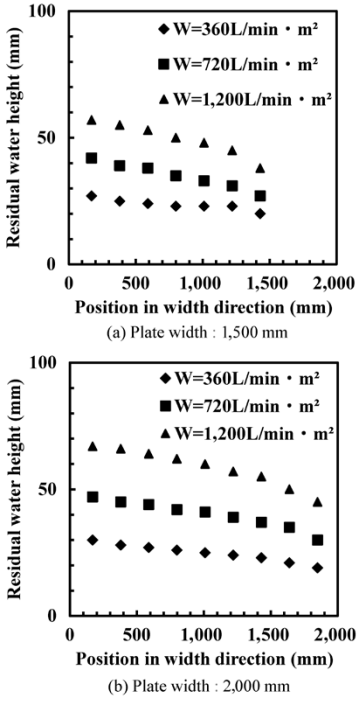

Fig. 3 Distribution of residual water height

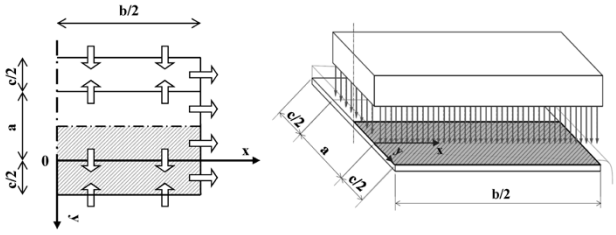

Fig. 4 Analysis model for residual water height prediction

The equations governing the analysis model are expressed by Equations (1) to (4).

The equations of continuity are given by Equations (1), (2):

for the nozzle injection region;

$$\partial(hu)/\partial x + \partial(hv)/\partial y = \gamma \quad \cdots\cdots (1)$$

for the non-nozzle-injection region;

$$\partial(hu)/\partial x - \partial(hv)/\partial y = 0 \quad \cdots\cdots (2)$$

The energy equation is given by Equation (3):

$$q^2 = (hu)^2 + (hv)^2 \quad \cdots\cdots (3)$$

The Bernoulli's equation is expressed by Equation (4):

$$H = h + (u^2 + v^2)/2g = h + q^2/2gh^2 \cdots\cdots (4),$$

wherein h is the height of residual water (m); u, the flow velocity in the x direction (m/s); v, the flow velocity in the y direction (m/s); γ, water flow density (m/s); q, water flow rate (m²/s); H, total head (m); g, the acceleration of gravity (m/s²).

The Bernouilli's equation holds only when the

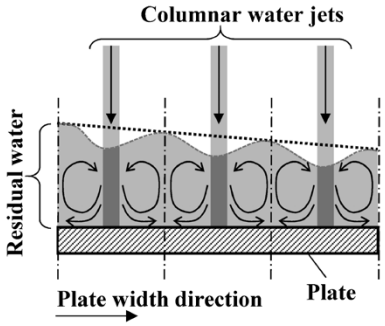

Fig. 5 Flow behavior in nozzle injection region

nozzle jet flow is mixed so as not to give friction to the flow from the upstream of residual water and cannot sufficiently express the flow behavior. Therefore, the flow behavior of the nozzle injection part (**Fig. 5**) is taken into account to expand Equation (4) so as to express the momentum redistribution and loss due to frictional force, as follows:

$$H = h + q^2/2gh^2 + Kq/gh \cdots\cdots (5)$$

wherein K is the friction coefficient (m/s).

Since q reaches the maximum at the position of $x = b/2$ and $y = 0$, the residual water height, h, becomes minimum at this position. Here, according to the concept of critical flow, $dq/dh = 0$ holds at the position of $x = b/2$ and $y = 0$, and Equation (5) becomes Equation (6):

$$h^3 - Hh^2 + q^2/2g + Kqh/g = 0 \cdots\cdots (6)$$

Thus,

$$(K/gh + q/g)(dq/dh) + 3h^2 - 2Hh + Kq/g = 0 \cdots\cdots (7)$$

Therefore, representing the critical flow by the subscript cr gives

$$3h_{cr}^2 - 2Hh_{cr} + kq_{cr}/g = 0 \quad \cdots\cdots (8)$$

$$h_{cr}^3 - Hh_{cr}^2 + kq_{cr}h_{cr}/g + q_{cr}^2/2g = 0 \quad \cdots\cdots (9)$$

wherein h_{cr} is the critical residual water height; q_{cr}, critical water flow rate.

Here, using a dimensionless constant, C, based on a dimensional analysis, the friction coefficient, K, is expressed by Equation (10):

$$K = Cq_{cr}/2h_{cr} \cdots\cdots (10)$$

wherein the critical residual water height, h_{cr}, the critical water flow rate, q_{cr}, and the total head, H, are given by Equations (11) to (13), respectively:

$$q_{cr} = \gamma(a/2)(b^2 + c^2)^{1/2}/(a + c) \cdots\cdots (11)$$

$$h_{cr} = \{(2 + C)q_{cr}^2/2g\}^{1/3} \cdots\cdots (12)$$

$$H = (3 + 2C)h_{cr}/(2 + C) \cdots\cdots (13)$$

The water flow rate q is given by Equations (14) and

(15):

$$q = \{2\gamma/(a+c)\}\ \{c^2(a/2+x)^2+(ay)^2\}^{1/2} : x < 0 \quad \cdots (14)$$

$$q = \{2\gamma/(a+c)\}\ \{a^2(c/2-x)^2+(ay)^2\}^{1/2} : x \geqq 0 \quad \cdots (15)$$

To determine the residual water height, h, it is necessary to find the roots of the cubic equation, Equation (6). Hence, taking Equation (16) into consideration, an approximate expression satisfying Equations (17) and (18) is derived as Equation (19):

$$dh/dq = -(Kh+q)/\{Kq+g(3h^2-2Hh)\} \quad \cdots\cdots (16)$$

$$h = H,\ dh/dq = -K/(gH) : q = 0 \quad \cdots\cdots (17)$$

$$h = h_{cr},\ dh/dq = -\infty : q = q_{cr} \quad \cdots\cdots (18)$$

$$h = h_{cr} + 2\{H - h_{cr} - Kq_{cr}/(gh)\}\{(1-q/q_{cr})^{1/2} - \{H - h_{cr} - 2Kq_{cr}/(gh)\}(1-q/q_{cr})\} \quad \cdots\cdots (19)$$

In particular, the measured value of the residual water height distribution in the width direction during the water model experiment is located at $y = c/2$, and q is expressed by Equation (20):

$$q = 2\gamma ax/(a+c) \quad \cdots\cdots (20)$$

Therefore, Equation (19) is expressed as Equation (21):

$$h = h_{cr} + 2\{H - h_{cr} - Kq_{cr}/(gH)\}(1-\alpha x)^{1/2} - \{H - h_{cr} - 2Kq_{cr}/(gH)\}(1-\alpha x) \quad \cdots\cdots (21)$$

$$\alpha = \{2\gamma a/(a+c)\}/q_{cr} = 4/(b^2+c^2)^{1/2} \quad \cdots\cdots (22)$$

The value calculated by Equation (21) and value measured were used to determine C. **Fig. 6** shows the measurement results and model prediction results for residual water height. As shown in this figure, the changes in residual water height with respect to the changes in water flow density and plate width can be predicted using the model equation, which is an expanded Bernoulli's equation.

1.2 Effect of residual water height on heat transfer characteristics

In the construction of the heat transfer model taking into account the residual water height, the effect of residual water height on heat transfer characteristics was examined by a cooling experiment using a down-sized apparatus simulating the cooling process used at Kobe Steel's steel plate mill(**Fig. 7**). The experimental apparatus consists of a heating furnace, a conveying table, a descaler, and a cooling header (**Fig. 8**). The descaler is a high-pressure water injection device for removing oxide scale, which is an influential factor

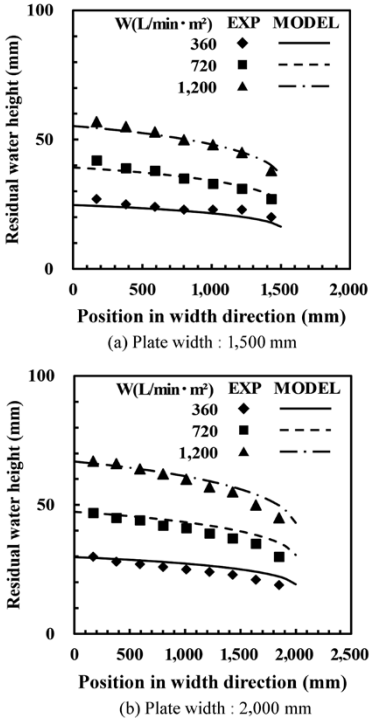

Fig. 6 Predicted and measured distributions of residual water height

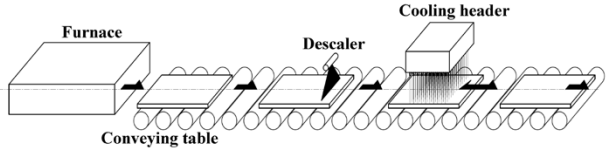

Fig. 7 Main components of small-sized apparatus for cooling experiment

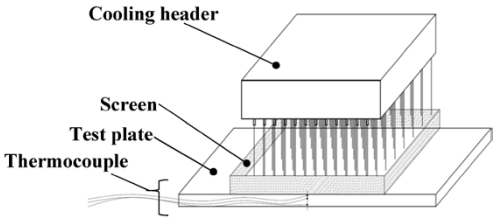

Fig. 8 Schematic of cooling header

in heat transfer characteristics. The cooling header is a cooling device with a group of columnar water jets nozzles. Here, the distance from the nozzle tip to the test plate was 300 mm, the nozzle diameter was 3 mm, the number of nozzles was 500 jets/m^2, and the header size was 500 × 500 mm. The residual water height was simulated by changing the height of the weir provided on the upper surface of the test plate. **Table 1** shows the set values of the weir height corresponding to each water flow density. The temperature of the test material was measured by thermocouples installed at multiple points in the thickness direction inside the plate.

In the cooling test, the test material was heated to 900℃ or higher in a heating furnace, taken onto the

Table 1 Relationship between water flow density and set value of screen height

Water flow density (L/min·m²)	Height of screen (mm)
200	0(Not set), 20
1,000	0(Not set), 40, 60
2,000	0 (Not set), 60, 100

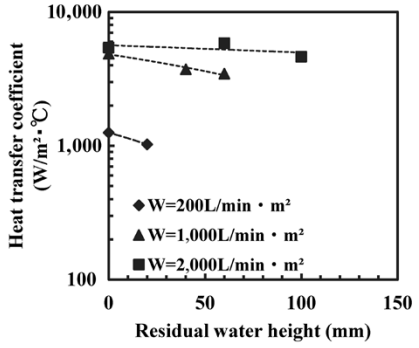

(a) Surface temperature in high temperature range:750 - 600℃

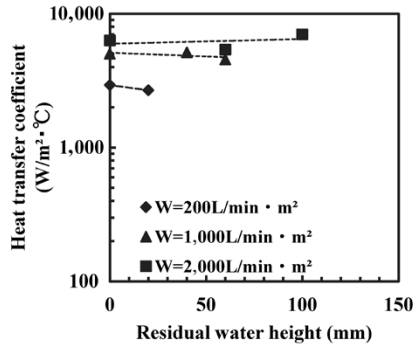

(b) Surface temperature in low temperature range:400 - 250℃

Fig. 9 Effect of residual water height on HTC (heat transfer coefficient)

transfer table, transferred to the descaler to remove the scale, and then transferred to the cooling header. The cooling was conducted by oscillate cooling in order to simulate the actual cooling process.

The heat-transfer coefficient, which is an evaluation index of heat transfer characteristics, was calculated by solving the inverse problem of the heat conduction equation at each temperature measurement point. **Fig. 9** shows the relationship between the heat-transfer coefficient and the calculated residual water height. This relationship confirms that the heat-transfer coefficient changes in accordance with water flow density and residual water height. When the water flow density is low (200 L/min・m²), the heat-transfer coefficient decreases as the residual water height increases, and this trend is observed in both the high temperature range (600℃ or higher) and the low temperature range (400℃ or lower). This is presumably because the impact pressure of the nozzle jet decreases with increasing residual water height.

On the other hand, when the water flow density is high (1,000 L/min・m², 2,000L/min・m²), only a small decrease in heat-transfer coefficient is associated with increasing residual water height. In particular, when the water flow density is 2,000 L/min・m², the heat-transfer coefficient becomes almost constant in the high temperature range regardless of the increase in residual water height. The results show only a slight increase in the heat-transfer coefficient in the low temperature range. This is presumably because the stirring effect of the residual water has been improved, although the collision pressure immediately below the nozzle jet has decreased with the increase of the residual water height. This trend has also been observed in experiments with a single cylindrical jet nozzle,[5] and similar results are obtained for the group of cylindrical jet nozzles.

A heat transfer model was constructed by combining these cooling test results with the residual water height model described in Section 1.1. The spray's cooling experimental equation[4] has been adapted for the basic model and has been expanded as shown in Equation (23), in consideration of the effect of residual water height on the heat transfer characteristics:

$$\log HTC = c_1 + c_2 \log W + c_3 T_s - d \log h \quad \cdots\cdots\cdots\cdots (23)$$

wherein HTC is the heat-transfer coefficient (W/m²・℃); W, water flow density (L/min・m²); T_s, steel plate surface temperature (℃); h, residual water height (m); and c_1, c_2, and c_3 are constants.

It should be noted that the residual water height, which affects the heat transfer characteristics, changes depending on the water flow density, and, therefore, the coefficient d is regarded as a function of water flow density.

In order to take into account the change in cooling capacity due to the boiling state of cooling water, the steel plate temperature was divided into two regions; i.e., high temperature region and low temperature region. The heat-transfer coefficient was formulated in each of these two temperature regions, and the two temperature regions were expressed by interpolating the respective equations.

In addition to the heat transfer model of the nozzle injection part described above, another heat transfer model was constructed for the non-nozzle-injection part between the cooling headers. That is, this model calculates the flow rate of the drainage flow from the center to the edge of the steel plate, which is in accordance with the residual water height distribution on the upper surface of the steel plate, on the basis of the difference in the residual water height, and thereby predicts the heat-transfer coefficient of the non-nozzle-injection part.

From these, the water flow density and the residual water height, which changes with the plate width at any position on the steel plate, can be predicted by a semi-theoretical equation. Hence, a heat transfer model has been constructed to predict the heat-transfer coefficient at any position of the steel plate, the coefficient that varies with the water flow density and the site on the steel plate.

2. Optimization of heat transfer model and accuracy evaluation

On the basis of the heat transfer model of the nozzle injection part on the upper surface of the steel plate described in section 1.2, heat transfer models were constructed for different areas (upper / lower cooling, nozzle injection part and non-nozzle-injection part) of the actual cooling header. Moreover, a temperature prediction model for cooling was constructed by combining the heat transfer models of the regions. The model parameters related to the influence factors, such as water flow density and steel plate surface temperature in the heat transfer model, have been determined by a cooling test using a small experimental apparatus. In order to compensate for the difference between the small experimental apparatus and the actual machine, the model parameters were optimized based on the temperatures measured at multiple points of the actual machine in the cooling process.

Fig.10 shows the values calculated by the temperature prediction model and the values measured. The multi-point measurement values obtained by adding the values measured for SCT and FCT and the temperature values measured [Note)] on the upper and lower surfaces of the steel plate in the recuperation process right after the cooling header were used as the basis for optimizing the model parameters such that the deviation between the calculated temperature values and the measured values was minimized. Since the cooling process is expressed by the heat transfer model for each region with different cooling conditions, it is necessary to set the model parameters for each region. For this reason, the model parameter was optimized using the particle swarm optimization (PSO) method,[7)] which is one of the optimization techniques for multi-variables, so as not to fall into local solutions.

Note) The measurements employed a normal thermometer for measuring the upper surface of a steel plate and a thermometer for measuring temperature on the lower steel plate surface introduced to actual machines.[6)]

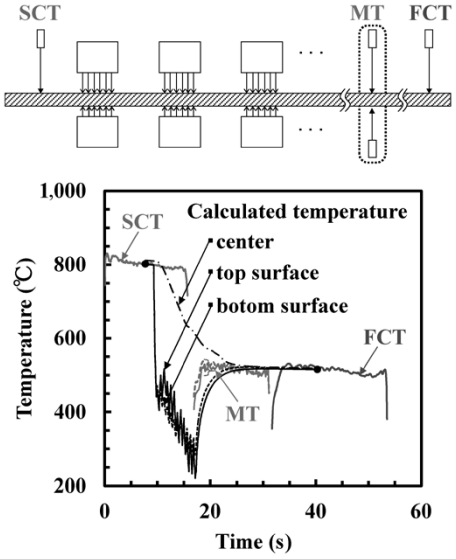

Fig.10 Calculated and measured temperatures

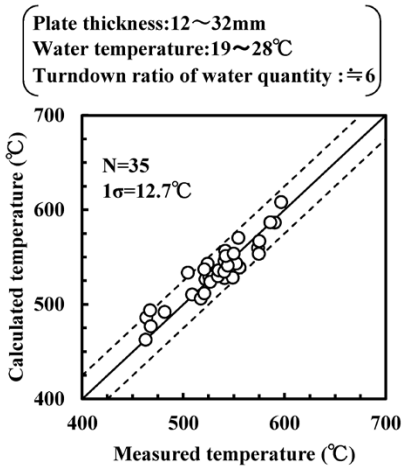

Fig.11 Calculated and measured FCTs

Fig.11 shows the calculated and measured values of the finishing cooling temperature based on the optimized temperature prediction model. Here, the prediction accuracy, 1σ, is 12.7℃. As the steel plate temperature decreases due to cooling, the boiling state transits from film boiling to nucleate boiling (transition boiling region). In the transition boiling region, the cooling capacity increases rapidly, making it difficult for conventional methods to predict the temperature. Therefore, a heat transfer model considering the flow state of the cooling water was used for the optimization based on the actual steel plate temperatures measured. This has enabled the prediction of the finishing cooling temperature with high accuracy even in the finishing cooling temperature range including cooling in the transition boiling region. **Fig.12** shows an example of the newly developed heat transfer model applied to the cooling control of an actual machine. The predictive values of temperature calculated by the heat transfer

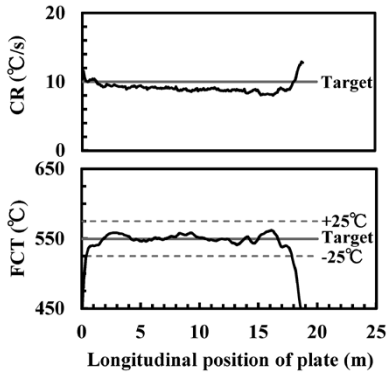

Fig.12 Results of online cooling control using developed heat transfer model (Plate thickness: 20 mm, FCT=550℃, CR=10℃/s)

model were used for setting the amount of cooling water satisfying the desired FCT and CR. Fig.12 shows the results of FCT and CR when the plate thickness is 20 mm, the target FCT is 550℃, and the target CR is 10℃/s. It is shown that highly accurate control has been realized with the FCT of the longitudinal steady-state portion of the steel plate, excluding the leading edge falling within ±25℃, and the CR for the same falling within ±1℃/s of the target value. Based on this, it has been confirmed that highly accurate temperature control is possible by applying the newly developed heat transfer model.

Conclusions

A study was conducted to improve the accuracy of the temperature control for steel plates in the accelerated-cooling header of Kakogawa Works steel plate mill. A prediction model for the height distribution of the cooling water on the upper surface of a steel plate was constructed along with a heat transfer model taking into account the flow state, the residual water height. The constructed heat transfer model was applied to the cooling control of an actual machine, which confirmed the feasibility of highly accurate temperature control.

Kobe Steel will work on to improve the control accuracy in a wide range of temperature control conditions and steel plate size conditions, and contribute to the commercialization, yield improvement and quality stabilization of new high-value-added steel plates.

References

1) I. Kozasu. Controlled Rolling · Controlled Cooling. Chijinshokan Co., Ltd. 1997.
2) Y. Serizawa et al. Nippon steel technical report. 2014, Vol.400, No.4, pp.18-25.
3) A. Fujibayashi et al. JFE Technical Report. 2004, No.5, pp.8-12.
4) Boiling heat transfer and cooling, The Japan Society of Mechanical Engineers. JAPAN INDUSTRIAL PUBLISHING CO., LTD. 1989.
5) Y. Haraguchi et al. CAMP-ISIJ. 2012, Vol.25, p.1042.
6) T. Ohara. CAMP-ISIJ. 2018, Vol.31, p.257.
7) Y. Oguma et al. Transactions of the Society of Instrument and Control Engineers. 2009, Vol.10, pp.512-521.